Three-dimensional visualization of fish morphometry and acoustic backscatter

J. Michael Jech

Northeast Fisheries Science Center, 166 Water St., Woods Hole, MA 02543
michael.jech@noaa.gov

John K. Horne

University of Washington, School of Aquatic and Fishery Sciences, Box 355020, Seattle, WA 98195
jhorne@u.washington.edu

Abstract: Theoretical acoustic models of fish are used to explain variability in backscatter measurements, improve estimation of target size, and improve target recognition and discrimination among acoustic targets. Acoustic backscatter models that incorporate fish morphology potentially provide more realistic predictions of echo amplitudes than models that approximate morphology using simple geometric shapes. Procedures to obtain digital representations of a fish's body and swimbladder are presented. These digital images are used in a Kirchhoff ray-mode model to predict backscatter amplitude as a function of fish length, acoustic frequency, and angle of insonification. Backscatter amplitude can be displayed as one-dimensional curves, two-dimensional response surfaces, and a three-dimensional backscattering surface (*i.e.*, ambit).

PACS numbers: 43.30.Gv, 43.30.Sf, 43.30.Ft
Date Received: 14 April 2001 **Date Accepted:** 21 October 2001

1. Introduction

Acoustic backscattering by fish depends on fish size, anatomical characteristics, morphology of the body and swimbladder, and location in the acoustic beam [*e.g.*, Foote, 1980]. Among teleost fish, swimbladders provide a large acoustic contrast compared to flesh or skeletal elements and are responsible for the primary (>90%) [Foote, 1980] contribution of backscattered sound. Anatomical attributes combined with organism behavior complicate the calculation of fish length from acoustic backscatter [Nakken and Olsen, 1977; Huang and Clay, 1980; Ehrenberg *et al*., 1981] and potentially influence the precision and accuracy of abundance or biomass estimates [Hawkins, 1981]. Empirical measures of backscatter as a function of fish length have been extensively studied [*e.g.*, MacLennan and Simmonds, 1992; Foote, 1991] and are used throughout the fisheries acoustics community. However, empirical measurements alone do not ensure accurate conversion of acoustic target strength to fish length. Modeling acoustic backscatter provides a quantitative tool to examine variability in backscatter measurements, improve estimation of target size, and improve discrimination among types of acoustic targets.

In this study, we outline steps to obtain digital representations of a fish's body and swimbladder and then use these digital images to predict acoustic backscatter using a Kirchhoff-ray mode (KRM) model [Clay and Horne, 1994]. Backscatter is predicted as a function of fish length, acoustic carrier frequency, and angle of insonification. Previous efforts have demonstrated reliable backscatter predictions at dorsal incidence (*e.g.*, Jech *et al.* [1995]; Horne *et al.* [2000]). We have initiated efforts to expand model calculations to include fish roll. Visualization of acoustic backscatter reveals both the potential and the limitations of the KRM model to predict backscatter at any spatial orientation.

2. Methods

Lateral and dorsal radiographs of an anaesthetized fish are used to construct digital representations of the fish body and swimbladder (Fig. 1). To convert radiograph images to digital data files, the body (excluding fins) and swimbladder silhouettes are traced on acetate.

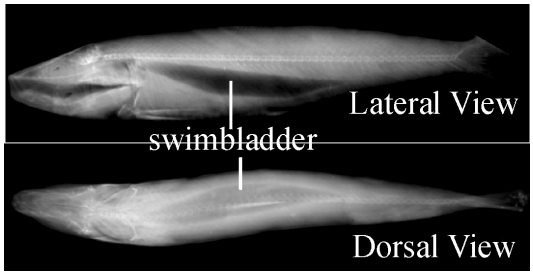

Fig. 1. Lateral (top) and dorsal (bottom) radiographs of a pilchard (*Sardinops ocellatus*). The swimbladder appears as a dark object relative to the skeletal structure. Note the angle of the dorsal surface of the swimbladder relative to the sagittal axis of the fish in the lateral view.

The maximum and minimum length and depth of the body and swimbladder are recorded to the nearest 0.5 mm, and the silhouette images are scanned into a computer graphics program. Separate digital images are created for the dorsal and lateral body views, as well as the dorsal and lateral swimbladder traces, taking care to retain the orientation of the swimbladder relative to the body. A digitizing program then reads the traces and scales the body parts to their true size using the maximum and minimum measurements (Fig. 2).

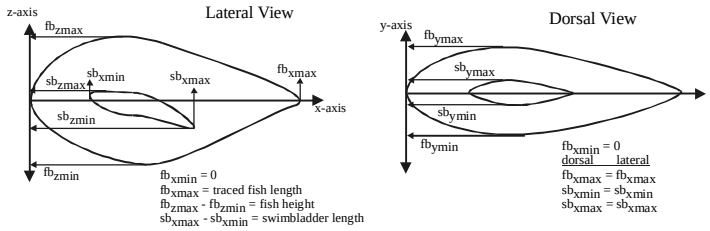

Fig. 2. Schematic showing locations of fish body (fb) and swimbladder (sb) lengths, heights, and widths for converting radiograph traces to digital files.

If necessary, trace lines are smoothed and rotated so that the sagittal axis of the fish body aligns with the x-axis. The fish body and swimbladder are digitized at 1 mm intervals along the sagittal axis, and the x, y, and z coordinates are tabulated in a data file. Current digitization preserves the true shape of the dorsal and ventral surfaces, but forces the body and swimbladder widths to be symmetric about the x-axis.

The Kirchhoff ray-mode (KRM) model partitions fish body and swimbladder morphometry into separate finite cylinders, computes the scattering from each cylinder, and then sums scattering over all cylinders to estimate total backscatter [Clay and Horne, 1994; Jech *et al*., 1995]. The digital fish body and swimbladder coordinates are used in the KRM model to predict acoustic backscatter as a function of insonifying frequency, fish length, and body angle relative to the incident wave front [Clay, 1991, 1992; Horne and Jech, 1999]. A web-based application (www.acoustics.washington.edu/krmmodel.html#comp_scat) provides interactive views of backscatter by the fish body, swimbladder and whole fish.

In this study, morphometric measurements and KRM model results from twelve Namibian pilchard (*Sardinops ocellatus*) are presented as examples of digital representation and backscatter prediction. These pilchard (total length range: 228-251 mm, standard length range: 195-221 mm) were sampled from a commercial purse seine catch and transported live to a veterinary clinic for morphometric and radiograph measurements during June 1999.

Mean and standard deviations of swimbladder and body lengths, depths (dorsal/ventral height), and widths were derived from the morphometric measurements (Table 1).

Table 1. Fish body and swimbladder morphometrics from 12 Namibian pilchard. Measurements are in mm, and length is standard length. Values in parentheses are one standard deviation from the mean. A colon (:) denotes the ratio.

	Fish Body	Swimbladder		
Mean Length	207.9 (7.6)	93.8 (6.2)	Body Length:Swimbladder Length	2.22 (0.11)
Mean Width	25.2 (4.5)	11.7 (2.9)	Body Width:Swimbladder Width	2.26 (0.54)
Mean Depth	40.4 (2.9)	10.2 (1.9)	Body Depth:Swimbladder Depth	4.05 (0.67)
Length:Width	8.52 (1.70)	8.74 (3.41)		
Length:Depth	5.16 (0.26)	9.47 (1.93)		

3. Acoustic Backscattering Predictions

The KRM model predicts a nonmonotonic relationship between backscatter amplitude and fish length (L) or acoustic wavelength (λ) (Fig. 3). The peaks and valleys along the backscatter curves are due to constructive and destructive interference between the carrier frequency and acoustic backscattering by the fish body and swimbladder (*e.g.*, 1 mm line in Fig. 3). KRM backscatter model predictions are sensitive to resolution of cylinder lengths (Fig. 3). Cylinder lengths were varied from 1 to 30 mm to examine the effect of digital resolution on backscatter amplitude. Amplitudes of backscatter curves are similar at low L/λ but diverge at higher L/λ with decreasing resolution and increasing carrier frequency. As the length of each cylinder increases, the accuracy of the digital image relative to the original morphometry decreases. Changing digital resolution results in small changes in the representation of the swimbladder or body. If image resolution is indicative of small movements in fish such as swimming behavior, then these model results suggest that variance in backscatter amplitudes is reduced at lower frequencies.

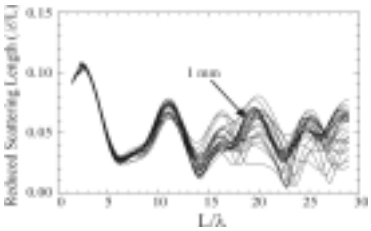

Fig. 3. Thirty predicted backscatter amplitude curves plotted as a function of the ratio of fish length (L) to acoustic wavelength (λ) at dorsal aspect ($\theta=90^o$). Reduced scattering lengths were predicted using the KRM model of a 217 mm Namibian pilchard (*Sardinops ocellatus*) at decreasing cylinder length resolutions of 1 mm to 30 mm.

KRM model predictions from several individuals of the same species can be combined to investigate intraspecific variability in backscattering amplitude. A backscatter response surface can be computed using backscatter predictions for a group of fish over specified fish tilt, length, and acoustic frequency ranges (Fig. 4). Tilt (θ) is the angle of the sagittal axis of the fish body relative to the incident wave front. The KRM model geometry sets $\theta=90^o$ where the sagittal axis of the fish body is parallel to the incident wave front. Peak backscatter amplitudes occur when the dorsal surface of the swimbladder is generally parallel to the incident wave front. For pilchard, peak amplitudes occur at approximately 80^o, which corresponds to the angle of the swimbladder axis relative to the body axis (cf. Fig. 1). The effect of fish tilt on backscatter amplitude is reduced at lower L/λ's (*i.e.*, flatter amplitude range across θ) when compared to higher L/λ's (*i.e.*, greater amplitude range). KRM backscatter predictions suggest that intraspecific variability in backscatter amplitude is dependent on tilt angle and acoustic frequency. For pilchard, greatest intra-specific echo

variability occurs ±10° from θ=80° and decreases as tilt angles diverge from θ=80°. These results also suggest that backscatter amplitudes from fish will be less variable when insonified at lower frequencies.

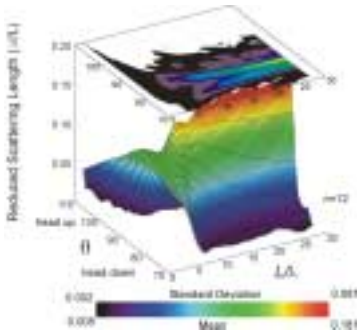

Fig. 4. Mean (lower surface) and standard deviation (upper contour) backscatter amplitudes of twelve Namibian pilchard (*Sardinops ocellatus*) plotted as a function of fish tilt (θ) and the ratio of fish length (L) to acoustic wavelength (λ). Reduced scattering lengths were predicted using the Kirchhoff-ray mode model. All fish were scaled to a length of 208 mm prior to calculations, and frequency was cycled from 12 to 200 kHz.

Expanding backscatter predictions from dorsal, ventral, or lateral surfaces to any spatial orientation requires a three-dimensional representation of the fish body and swimbladder. To recreate three-dimensional volumes of the fish body and swimbladder, elliptical or circular interpolation is used between the dorsal and lateral digital images. With elliptical interpolation, the endpoints are located at the dorsal and ventral surfaces (note that although elliptical interpolation can be used to obtain fish morphometry, the KRM model uses equivalent cylinders to predict backscatter). A mesh is created using a resolution of cylinder length along the fish axis and equally spaced roll points (Fig. 5).

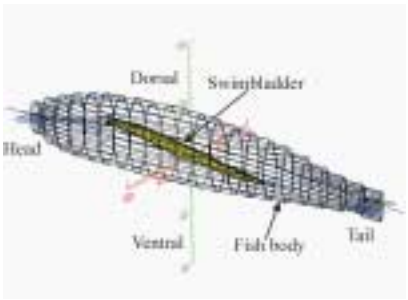

Fig. 5. Cylindrical representation of a 207 mm pilchard body and swimbladder used in Kirchhoff-ray mode backscatter model. The swimbladder is tilted approximately 10° posterior relative to the sagittal axis of the fish. Axes units are in mm, cylinder lengths are 10 mm for the fish body and 2 mm for the swimbladder. Roll points are at 15° intervals.

The KRM model can then be used to predict backscatter amplitude for 360° of tilt and roll to produce a three-dimensional backscattering surface (backscattering ambit, Fig. 6). Visualization of the backscattering ambit (Fig. 6 and Mm.1) graphically depicts the effects of fish roll and tilt on echo amplitude.

Mm.1. Fancy video file (3.4Mb)

Because the Kirchhoff approximation is theoretically limited to angles near broadside incidence (*e.g.*, Clay and Horne [1994]; Partridge and Smith [1995]), aspect angles within 60° of head- and tail-on aspects are displayed as gray and aspect angles within 30° of dorsal/ventral or lateral incidence are color-coded. For pilchard, peak dorsal amplitude

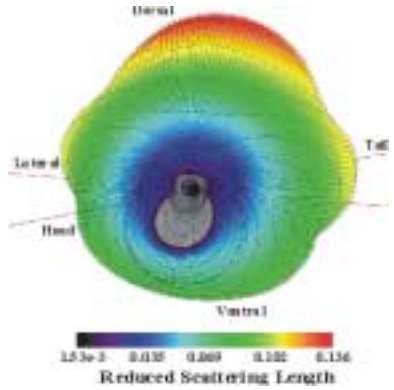

Fig. 6. Acoustic backscatter ambit of a 207 mm pilchard at 38 kHz. Backscatter amplitude is represented as distance from the center of the axes and color-coded using red for high amplitude and blue for low amplitude. Grayed portions of the ambit ($\pm 60^o$ from head- and tail-on aspects) denote predicted amplitudes that are less reliable. Reduced scattering length is resolved at 2^o in the tilt plane and 2^o in the roll plane. Maximum amplitude occurs when the swimbladder is orthogonal to the incident wave front, which tilts the fish approximately 10^o head down.

occurs at approximately 80^o, which corresponds to a head down tilt angle of 10^o. Echo amplitudes at head- and tail-on aspects are significantly reduced from lateral or dorsal incidences. The lateral symmetry in the scattering ambit is due, at least in part, to the digital representation of the swimbladder and fish body. Each backscattering ambit is calculated at a specified frequency, as we have yet to determine how to visualize multiple frequencies simultaneously. As L/λ increases (not shown), the number of features such as "ridges" and "folds", in the backscattering ambit increases similar to the backscattering surface in Fig. 4.

4. Discussion

Computer visualizations of acoustic backscatter can be used to quantify the effects of fish behavior, fish length, and acoustic frequency on echo amplitudes. Interactive representations of fish body and swimbladders used in the KRM model, and the resulting acoustic backscattering response curves, surfaces, and ambits are now available on the web (www.acoustics.washington.edu). Data visualizations should prompt the viewer to think about mechanisms that cause patterns observed in data, present large data sets in a coherent and comprehensive manner, reveal several levels of detail without distortion, and encourage comparison among different data sets [Tufte, 1983].

The KRM model and current three-dimensional realizations of fish body and swimbladder morphometry have limitations. Dorsal and lateral views provide two planes to derive three-dimensional representations. Ideally, three-dimensional imaging techniques such as CAT scans or flash freezing and reconstructing microtomed sections [Foote, 1985; Ona, 1990] could be used to obtain an accurate representation of morphology. At this time we do not know the degree of anatomical detail required to maximize accuracy of model predictions. Inexpensive and accessible imaging methods are needed to obtain accurate and complete three-dimensional images of a fish's swimbladder and internal structures (*e.g.*, gonads). As digital imaging technology becomes more accessible to fisheries researchers, the ability to characterize effects of body forms, ontological changes, and gonad development on acoustic scattering will improve (*e.g.*, Barr, 2001). The KRM model computes backscattering from the incident surface of equivalent cylinders. Comparisons of laboratory measurements and KRM model predictions are robust and reliable for angles near dorsal or lateral incidence [Clay and Horne, 1994; Jech *et al.*, 1995]. The current approximation of body and swimbladder morphology using equivalent cylinders make KRM model predictions at

insonifying angles near head- and tail-on less reliable. Expanding the KRM model and/or further investigation into other models (*e.g.*, finite element boundary element [Foote, 1985] or conformal mapping [Diperna and Stanton, 1994]) may be required to achieve accurate model predictions at all orientations.

This study describes a step in the evolution of acoustic modeling and visualization of acoustic backscatter. To extend the ability to estimate abundance, biomass, and lengths for other underwater acoustic technologies, such as omnidirectional or multibeam SONARs, estimates of the backscattering cross-section of individuals at any spatial orientation must be obtained. The combination of acoustic modeling with *in situ* and laboratory measurements is the best strategy to quantify variability in acoustic estimates used in fisheries assessments. Model innovations may enable the 'scaling-up' of predictions from individuals to aggregations, and the prediction of ontological and reproductive effects on backscatter amplitudes.

Acknowledgment

This work was supported by Office of Naval Research Divisions of Acoustical Oceanography and Biological/Chemical Oceanography. The authors would like to thank Drs. Ole Misund and John Dalen (Institute of Marine Research, Bergen, Norway) for the invitation to participate on a Namibian cruise aboard the Dr. Fridtjof Nansen and for constructive advice during formulation of the visualizations. The authors also thank Rick Towler for the animation, Elliott Hazen for swimbladder measurements, and an anonymous reviewer and the associate editor for insightful comments to clarify this paper.

References and links

Barr, R. **(2001)**. "A design study of an acoustic system suitable for differentiating between orange roughy and other New Zealand deep-water species," J. Acoust. Soc. Am. **109,** 164-178.

Clay, C.S. **(1991)**. "Low-resolution acoustic scattering models: Fluid-filled cylinders and fish with swimbladders," J. Acoust. Soc. Am. **89**, 2168-2179.

Clay, C.S. **(1992)**. "Composite ray-mode approximations for backscattered sound from gas-filled cylinders and swimbladders," J. Acoust. Soc. Am. **91**, 2173-2180.

Clay, C.S., and Horne, J.K. **(1994)**. "Acoustic models of fish: The Atlantic cod (*Gadus morhua*)," J. Acoust. Soc. Am. **96**, 1661-1668.

DiPerna, D.T., and Stanton, T.K. **(1994)**. "Sound scattering by cylinders of noncircular cross section: A conformal mapping approach," J. Acoust. Soc. Am. **96**, 3064-3079.

Ehrenberg, J.E., Carlson, T.J. Traynor, J.J., and Williamson, J.J. **(1981)**. "Indirect measurement of the mean backscattering cross section of fish," J. Acoust. Soc. Am. **69**, 955-962.

Foote, K.G. **(1980)**. "Averaging of fish target strength functions," J. Acoust. Soc. Am. **67**, 504-515.

Foote, K.G. **(1985)**. "Rather-high-frequency sound scattering by swimbladdered fish," J. Acoust. Soc. Am. **78**, 688-700.

Foote, K.G. **(1991)**. "Summary of methods for determining fish target strength at ultrasonic frequencies," J. Cons. Int. Explor. Mer. **48**, 211-217.

Hawkins, A.D. **(1981)**. "Some biological sources of error in the acoustical assessment of fish abundance," in *Meeting on Hydroacoustical Methods for the Estimation of Marine Fish Populations*, edited by J.B. Suomola (Draper Laboratories, Cambridge, Massachusetts).

Horne, J.K. and Jech, J.M. **(1999)**. "Multi-frequency estimates of fish abundance: constraints of rather high frequencies," ICES J. Mar. Sci. **56**, 184-199.

Horne, J.K., Walline, P.D., and Jech, J.M. **(2000)**. "Comparing acoustic model predictions to *in situ* backscatter measurements of fish with dual-chambered swimbladders," J. Fish Biol. **57**, 1105-1121.

Huang, K., and Clay, C.S. **(1980)**. "Backscattering cross-sections of live fish: PDF and aspect," J. Acoust. Soc. Am. **67**, 795-802.

Jech, J.M., Schael, D.M., and Clay, C.S. **(1995)**. "Application of three sound scattering models to Threadfin Shad (*Dorosoma petenense*)," J. Acoust. Soc. Am. **98**, 2262-2269.

MacLennan, D. N., and Simmonds, E.J. **(1992)**. *Fisheries Acoustics* (Chapman and Hall, London).

Nakken, O., and Olsen, K. **(1977)**. "Target strength measurements of fish," Rapp. P.-v. Réun. Cons. Int. Explor. Mer **170**, 53-69.

Ona, E. **(1990)**. "Physiological factors causing natural variations in acoustic target strength of fish," J. Mar. Biol. Ass. U.K. **70**, 107-127.

Partridge, C., and Smith, E.R. **(1995)**. "Acoustic scattering from bodies: Range of validity of the deformed cylinder method," J. Acoust. Soc. Am. **97**, 784-795.

Tufte, E.R. **(1983)**. *The Visual Display of Quantitative Information* (Graphics Press, Cheshire, Connecticut).